Amirkabir University of Technology
(Tehran Polytechnic)

Amirkabir International Jounrnal of Science & Research
Electrical & Electronics Engineering
(AIJ-EEE)
Vol. 48, No. 2, Fall 2016, pp. 81-91

Adaptive Fusion of Inertial Navigation System and Tracking Radar Data

M. Fathi[1,*], N. Ghahramani[2], M. A. S. Ashtiani[3], A. Mohammadi[4], M. Fallah[5]

1- Ph.D. Candidate, Department of Aerospace Engineering-Flight Mechanics and Control Group, Malek Ashtar University of Technology
2- Associate Professor, Department of Electrical Engineering-Control Group, Malek Ashtar University of Technology
3- Associate Professor, Department of Aerospace Engineering-Flight Mechanics and Control Group, Malek Ashtar University of Technology
4- Assistant Professor, Department of Electrical Engineering-Control Group, Malek Ashtar University of Technology
5- Assistant Professor, Department of Electrical Engineering-Communication Group, Malek Ashtar University of Technology

(Received 10 October 2015, Accepted 29 May 2016)

ABSTRACT

Against the range-dependent accuracy of the tracking radar measurements including range, elevation and bearing angles, a new hybrid adaptive Kalman filter is proposed to enhance the performance of the radar aided strapdown inertial navigation system (INS/Radar). This filter involves the concept of residual-based adaptive estimation and adaptive fading Kalman filter, and tunes dynamically the filter parameters, including the fading factors and the measurement and process noises scaling factors based on the ratio of the actual residual covariance to the theoretical one. In fact, due to the unknown and fast-varying statistical parameters of the radar measurement noises and their nonlinear characteristics, applying a conventional Kalman filter to INS/Radar fusion yields a low-performance navigation and in-flight alignment. The Monte Carlo simulation results of the integrated navigation system on an interceptor missile trajectory indicate the new algorithm has an effective performance in the face of nonlinearities and uncertainties of the tracking radar measurements. These results allow knowing whether the fine in-flight alignment and high-performance navigation can be possible for the long-range air defense missile using the low-cost INS/Radar system without aiding global navigation satellite system signals.

KEYWORDS:

Adaptive Kalman Filter, Inertial Navigation, In-flight Alignment, Radar

Please cite this article using:
Fathi, M., Ghahramani, N., Ashtiani, M. A. S., Mohammadi, A., and Fallah, M., 2016. "Adaptive Fusion of Inertial Navigation System and Tracking Radar Data". *Amirkabir International Journal of Electrical and Electronics Engineering*, 48(2), pp. 81–91.
DOI: 10.22060/eej.2016.818
URL: http://eej.aut.ac.ir/article_818.html
*Corresponding Author, Email: mahd_fathi@mut.ac.ir

1- Introduction

It is widely accepted that the modern long-range air defense missiles will require a two-phase guidance strategy employing a mid-course phase followed by terminal homing. These tactical missiles will require an on-board strapdown inertial navigation system, INS, to perform the functions, such as the provision of the data for a navigation of the missile prior to a period of terminal homing, provision of homing head pointing commands and provision of autopilot feedback signals [1].

Due to INS intrinsic defect and special mission of an anti-air missile, four problems can appear. First, INS navigation errors propagate as a result of instrument errors, initial alignment error, and imperfections in the strapdown computing algorithms. Second, many air defense missiles require an accurate alignment of the onboard INS in order to achieve a high probability of killing against their intended targets [2]. Third, air defense systems require rapid reaction time, thus significant pre-launch delays for alignment are not tolerable [2]. Fourth, typically, such tactical systems require medium grade inertial quality instruments (high cost) to carry out their functions and to ensure an accurate transition to the terminal phase of flight.

As a solution to overcoming these problems, the tracking radar (radio detection and ranging) aided INS was presented in [1,3]. In this particular application, the launch platform can provide only a very coarse initialization for the missile's INS then the missile is fired to intercept an intended target. The missile and the target are tracked by a ground-based radar system. The radar provides measurements of missile range, elevation and bearing with respect to the radar set. These measurements may be passed to the missile via an uplink transmitter and used to aid the on-board INS. The missile on-board inertial navigation system implements a Kalman filter to determine in-flight corrections to the navigation errors.

Several studies have been conducted on INS/Radar to gain the benefits of in-flight alignment of INS, in-flight calibration of INS, improvement of INS performance and in-flight registration of radar frame with navigation frame.

Both the in-flight alignment by INS/Radar integration and the pre-launched alignment by shipboard measurements for a ship launched missile's INS are developed and their relative merits are compared in [1]. The subject of [2-8] is related to the development of a radar and GPS (global positioning system) aided INS for a navy tactical ballistic missile defense interceptor missile (Standard Missile SM-3). An overview and a preliminary performance assessment of an INS/Radar/GPS system based on a direct Kalman filter with 20 states are provided in [3]. The research in [2,4] proposes a new metric to determine the degree of observability of attitude errors in flight alignment of INS/Radar/GPS over specified missile flight profiles. In-flight alignment of an onboard INS using the external radar and GPS data and a conventional Kalman filter for data fusion have been explained in detail in [5,6]. Sure enough, a cornerstone to the in-flight alignment was laid out in [7-9] which addressed the question: what kind of horizontal maneuver is preferable in the in-flight INS alignment; the interested reader is directed to these references for a more detailed discussion of in-flight alignment. The references [10,11] discuss the successful flight test results of the INS/Radar/GPS system for the missile SM-3. A strapdown INS augmentation scheme comprising astronavigation system and secure radio positioning system is proposed in [12]. Also, the issue of the Mars entry navigation using integration of information sensed from radio beacons and information derived from inertial measurement unit is addressed in [13].

All the above-mentioned researches relevant to the integration of INS and radar data assume that the measurement noise covariance matrix (R) in the Kalman filter is fixed. In other words, it is supposed that the tracking radar measurements have constant standard deviations. However, it is well known that the radar measurements accuracies are very range depended [14, chapter 11], [15, chapter 4]. Indeed, the accuracies of range and angles (elevation and bearing) measured by the radar are the functions of the range (see section 2 for the details). It means the matrix R should be a varying matrix, not a fixed one.

Insufficient a priori information about this varying matrix R affects the accuracy of the INS/Radar integrated system. In fact, insufficiently known a priori filter statistics will reduce the precision of the estimated filter states or introduce biases to their estimates [16]. In addition, wrong a priori information will lead to the practical divergence of the filter. For example, if R is too small at the beginning of the estimation process, the uncertainty tube around the true value in a probabilistic sense will tighten and a biased solution will result. If R is too large, a filter divergence, in the statistical sense could be resulted.

Besides, it will result in a longer estimation transition for the filter whose total operation time is very short (about 1 to 3 minutes for a long-range air defense missile flight). These minute points imply that using a fixed filter designed by conventional methods for an INS/Radar system with the changing radar measurements accuracies is a major drawback.

From this point of view, this study proposes that the fixed estimation formulation for the INS/Radar integrated system has resulted in a poor estimation performance and should be replaced by an adaptive estimation filter with a varying measurement noise covariance matrix. It can be expected that with the adaptive fusion scheme, a better navigation performance can be achieved.

The paper is organized as follows. In section II, the tracking radar is introduced and the measurement errors of a specific tracking radar are analyzed. Section III outlines the residual-based adaptive estimation / the adaptive fading Kalman filter hybrid method (RAE/AFKF) which is the main contribution of this paper. In section IV, the process and measurement model for INS/Radar integration system are provided. In section V, the performance of RAE/AFKF is evaluated in Monte Carlo simulations compared with an extended Kalman filter, EKF. Finally, section VI provides concluding remarks.

2- An assessment of tracking radar measurement errors

A typical tracking radar has a pencil beam to receive echoes from a single target and tracks the target in angle, range, and/or doppler. Discussion in [15, chapter 4] and [17, chapters 8, 9] shows that the several major effects on the accuracy of the tracking radar measurements are as follows:

- Glint, or angle noise which affects all the tracking radars especially at a short range. The error due to glint varies inversely with the range.
- Receiver noise which also affects all the radar types, and mainly determines to track accuracy at the long range. The receiver noise causes the error to vary as the square of the range.
- Amplitude fluctuations of the target echo that bother the conical-scan and sequential lobing type of radars, but not the monopulse type. The amplitude fluctuations effect is independent of the range.
- Clutter and multipath effects;
- Servo noise and servo lag of tracking mechanism; the servo noise is independent of the range.

The contribution of glint, receiver noise and amplitude fluctuations to the accuracy of a tracking radar as a function of range is illustrated in Fig. 1.

Fig. 1 is a very qualitative plot showing the general nature of each of these factors, while precise investigations of tracking errors associated with a particular monopulse phased-array radar system and with the radar AN/FPS-16 are discussed and presented in [18] and [14, page 11-12], [19, pages 48-94], respectively. But the specific operating conditions assumed in [14,18,19], such as the target radar cross section, RCS, and altitude are not compatible with what this research needs. Thus, based on the free-space performance analysis and the missile target RCS, standard deviation (STD) of the total angle and range errors of the tracking radar An/FPS-16 as a function of range are roughly estimated as illustrated in Figs. 2 and 3 (see appendix A for the radar equations). Although this radar is one of the early monopulse radars, it remains in a wide use and represents one of the most accurate tracking devices employed in the test-range instrumentation. Its major parameters are listed in [17, pages 542-543].

3- INS/Radar adaptive integration system

As mentioned in section I, due to the unknown range-varying statistical parameters of the radar measurement noises, applying the EKF to INS/Radar integration results in a low-performance estimation. In order to enhance its performance, this unknown and variable statistical parameter needs to be estimated and adapted with the system state and the error covariance. Two popular types of the adaptive Kalman filter algorithms include the innovation-based adaptive estimation, IAE, approach and the

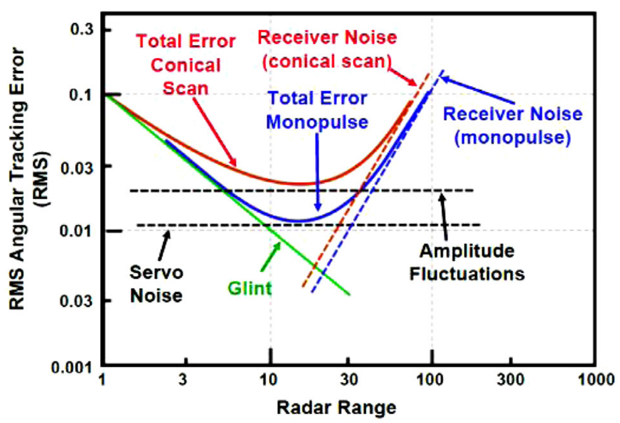

Fig. 1. Qualitative plot showing relative contributions to the angle tracking error without units [15, page 235]

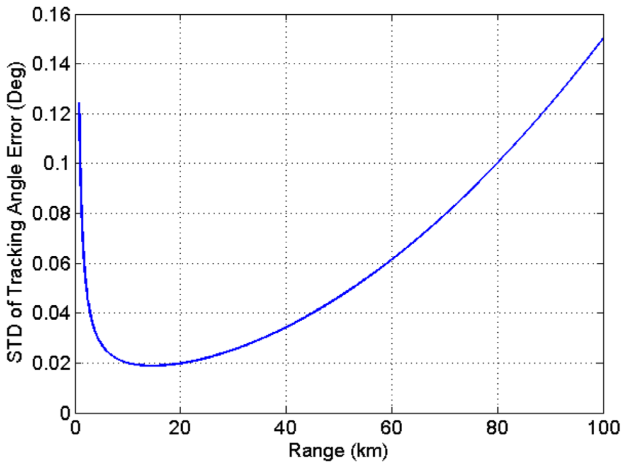

Fig. 2. A rough estimation of the tracking angle error STD for the AN/FPS-16 in the free-space analysis

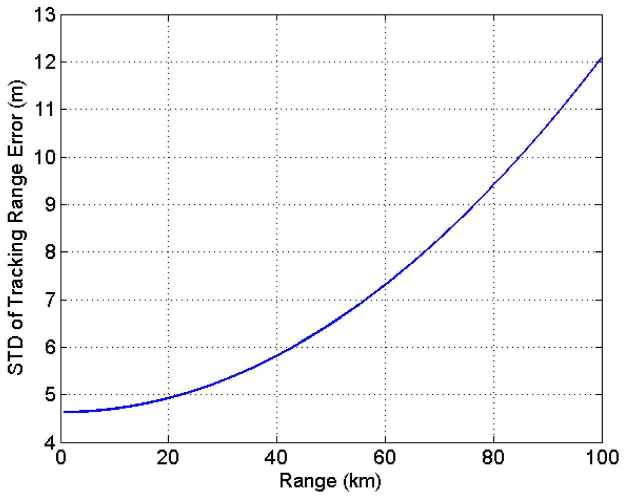

Fig. 3. A rough estimation of the tracking range error STD for the AN/FPS-16 in free-space analysis

adaptive fading Kalman filter, AFKF, approach [20]. The innovation sequences in IAE method have been utilized by the correlation and covariance-matching techniques to estimate the noise covariance. The basic idea behind the covariance-matching approach is to make the actual value of the covariance of the innovation consistent with its theoretical value. The implementation of IAE-based adaptive Kalman filter, IAKF, to navigation designs has been widely explored in [16,21]. The idea of AFKF is to incorporate suboptimal fading factors as a multiplier into the predicted covariance matrix to deliberately increase the variance of the predicted state vector to enhance the influence of innovation information and improve the tracking capability in high dynamic maneuvering [22].

In this study, the methods IAKF, AFKF and the hybrid approach IAE/AFKF developed in [23] were applied to INS/Radar integration problem as none of them solely was able to satisfy the desired performance. Therefore, a new hybrid approach involving the concept of residual-based adaptive estimation, RAE, and AFKF is presented. The ratio of the actual residual covariance based on the sampled sequence to the theoretical residual covariance will be employed for dynamically tuning three filter parameters, including fading factor (λ_P), measurement noise scaling factor (λ_R) and process noise scaling factor (λ_Q). To provide these factors, the Kalman filter approach is coupled with the adaptive tuning system, ATS. In the ATS mechanism, the adaptations on the error states covariance matrix (P), on process covariance matrix (Q) and on the measurement noise covariance are involved. The idea is based on the concept that when the filter achieves estimation optimality, the actual residual covariance based on the sampled sequence and the theoretical residual covariance should be equal.

3- 1- Integration algorithm

As shown in Fig. 4, the position states of INS, i.e. x, y, z, may be compared with the same quantities obtained from a radar model. This model converts the radar measurements of the radar Polar coordinate system into the radar Cartesian one using $x=R\cos\Theta\sin\Psi$, $y=R\cos\Theta\sin\Psi$ and $z=-R\sin\Theta$ where R, Θ and Ψ are range, elevation, and bearing, respectively.

The differences between the actual and predicted measurements are the filter measurements innovations. These quantities are multiplied by the Kalman gains to provide estimates of the errors in the INS indicated position, velocity, and attitude. Also, because of insufficient knowledge of the radar measurement noise statistics, a residual-based adaptive tuning system effectively adapts R, Q and

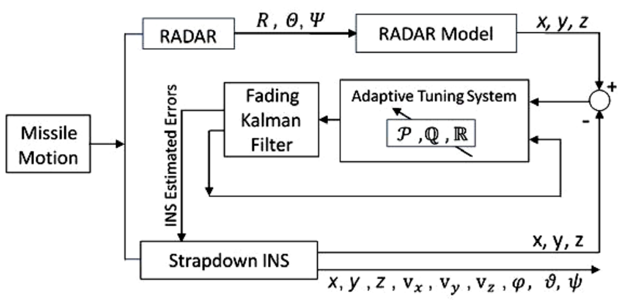

Fig. 4. INS/Radar System Block Diagram

P to compensate such lack of information. Finally, the estimates of the errors are subsequently used to correct the INS solutions over time, and update takes place following the arrival of each radar measurement of the missile positions.

3- 2- ARAE/AFKF hybrid algorithm

The process model and measurement model are represented [24, chapter 4] as:

$$x_k = \mathcal{F}_{k-1} x_{k-1} + \mathbf{G}_{k-1} \mathbf{w}_{k-1} \quad (1)$$

$$z_k = \mathcal{H}_k x_k + \mathbf{M}_k \boldsymbol{v}_k \quad (2)$$

where the state vector $x_k \in R^n$, process noise vector $w_k \in R^n$, measurement vector $z_k \in R^m$, and measurement noise vector $v_k \in R^m$. In Eqs. (1) and (2), both the vectors w_k and v_k are zero mean Gaussian white sequences having zero cross-correlation with each other:

$$E\left(\boldsymbol{w}_k \boldsymbol{w}_j^T\right) = \mathbb{Q}_k \delta_{k-j} \quad (3)$$

$$E\left(\boldsymbol{v}_k \boldsymbol{v}_j^T\right) = \mathbb{R}_k \delta_{k-j} \quad (4)$$

$$E\left(\boldsymbol{w}_k \boldsymbol{v}_j^T\right) = 0 \quad (5)$$

where Q_k is the process noise covariance matrix, R_k is the measurement noise covariance matrix, F is the state transition matrix, E [.] represents expectation and superscript "T" denotes matrix transpose. From the measured z_k and the predicted measurement $\hat{z}_k^+ = H_k x_k^+$ based on the updated filter states x_k^+, the residuals sequence is defined as $v_k = z_k - \hat{z}_k^+$. Also, the theoretical covariance matrix of the residual sequence, developed in [16], is given by:

$$\mathbf{C}_{v_k} = E\left[v_k v_k^T\right] = \mathbb{R}_k - \mathcal{H}_k \mathcal{P}_k^+ \mathcal{H}_k^T \quad (6)$$

Defining $\hat{C}_{v_k}$ as the statistical sample variance estimate of C_{v_k}, matrix $\hat{C}_{v_k}$ can be computed by averaging inside a moving estimation window of size N:

$$\hat{C}_{v_k} = \frac{1}{N} \sum_{j=j_0}^{k} v_k v_k^T \quad (7)$$

where N is the number of samples (usually referred to the window size); $j_0 = k - N + 1$ is the first sample inside the estimation window. The window size N is chosen empirically to give some statistical smoothing.

The block diagram of RAE/AFKF hybrid method and further details regarding the residual-based adaptive tuning system loop are illustrated as a flow chart in Fig. 5.

where P_k is the error covariance matrix defined by $E[(x_k - \hat{x}_k)(x_k - \hat{x}_k)^T]$, in which $\hat{x}_k$ is an estimation of the system state vector x_k, and the weighting matrix K_k is generally referred to as the Kalman gain matrix. Also, the value $0 < \alpha \leq 1$ is determined empirically through computer simulation.

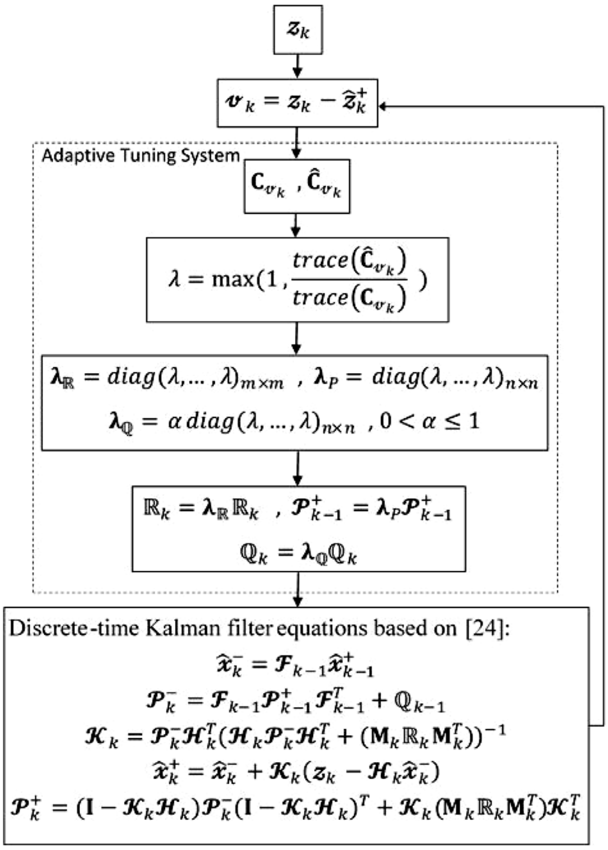

Fig. 5. Block Diagram of RAE/AFKF for an Adaptive Estimation

4- Mathematical modeling

In this section, linear differential equations of the INS are derived and are presented as the process model. Also, the measurement model based on the difference between the radar and the INS measurements is obtained.

4- 1- Process modeling

The tangent coordinate frame (t-frame) is defined to be an earth-fixed which is aligned with a geographic frame at the fixed location missile launcher on the earth. In this system, the navigation equations are [25, chapter 3]:

$$\dot{\mathbf{r}}^t = \mathbf{v}^t \quad (8)$$

$$\dot{\mathbf{v}}^t = \mathbf{C}_b^t \mathbf{f}_b - \left(2\boldsymbol{\omega}_{it}^t \times \mathbf{v}^t\right) + \mathbf{g}_l^t \quad (9)$$

$$\dot{\mathbf{C}}_b^t = \mathbf{C}_b^t \boldsymbol{\Omega}_{tb}^b \quad (10)$$

where ω_{it}^t is the turn rate of the earth expressed in the t-frame:

$$\boldsymbol{\omega}_{it}^{t} = \left[\Omega \cos L_f \;\; 0 \;\; -\Omega \sin L_f\right]^T \quad (11)$$

L_f, Ω and $\mathbf{f}_b$ represent latitude of the missile launcher location, earth's rate, and the specific force in the missile body frame, respectively. Also ω_{tb}^{b} is the turn rate of the body with respect to the t-frame; Ω_{tb}^{b} is the skew-symmetric form of ω_{tb}^{b}, C_b^t which is a direction cosine matrix to transform the measured specific force vector to navigation axes (t-frame) and g_l^t represents the gravity field vector.

The linearized differential Eqs. (8) to (10) are:

$$\begin{bmatrix} \delta\dot{\mathbf{r}}^t \\ \delta\dot{\mathbf{v}}^t \\ \dot{\phi} \\ \dot{\boldsymbol{\varepsilon}} \end{bmatrix} = \begin{bmatrix} 0 & I & 0 & 0 \\ \mathbf{A}_{21} & \mathbf{A}_{22} & \mathbf{A}_{23} & 0 \\ 0 & 0 & A_{33} & 0 \\ 0 & 0 & 0 & 0 \end{bmatrix} \begin{bmatrix} \delta\mathbf{r}^t \\ \delta\mathbf{v}^t \\ \phi \\ \boldsymbol{\varepsilon} \end{bmatrix} + \begin{bmatrix} 0 & 0 & 0 & 0 \\ 0 & \mathbf{C}_b^t & 0 & 0 \\ 0 & 0 & -\mathbf{C}_b^t & 0 \\ 0 & 0 & 0 & 0 \end{bmatrix} \begin{bmatrix} 0 \\ \mathbf{w}_a \\ \mathbf{w}_g \\ 0 \end{bmatrix} \quad (12)$$

$$\mathbf{A}_{21} = \mathbf{G} - \left[\boldsymbol{\omega}_{\mathrm{it}}^{\mathrm{t}} \times\right]\left[\boldsymbol{\omega}_{\mathrm{it}}^{\mathrm{t}} \times\right] \quad (13)$$

$$\mathbf{A}_{22} = -2\left[\boldsymbol{\omega}_{\mathrm{it}}^{\mathrm{t}} \times\right] \quad (14)$$

$$\mathbf{A}_{23} = \left[\mathbf{f}^{\mathrm{t}} \times\right] \quad (15)$$

$$\mathbf{A}_{33} = -\left[\boldsymbol{\omega}_{\mathrm{it}}^{\mathrm{t}} \times\right] \quad (16)$$

where $\mathbf{G}$ and g^n are the gravity gradient matrix and the gravity vector referenced in the local level geographic frame (n-frame), respectively. Although $\mathbf{G}$ may be negligible for a low cost or tactical grade INS, in Appendix B a new model for $\mathbf{G}$ is derived. $\delta\mathbf{r}^t$ and $\delta\mathbf{v}^t$ are the INS position and velocity errors, and ϕ is the body-to-navigation attitude error. ε is defined as the error vector in the transformation between the radar face and navigation coordinate frames. The components of ε are the misalignment errors between them as shown in Fig. 6. Superscripts or subscripts t, R and b denote the tangent, radar and body frames, respectively. $\mathbf{w}_a$ and $\mathbf{w}_g$ are accelerometers and gyros noise vector. Eq. (12) in discrete-time domain takes the form Eq. (1) using the error state vector expressed in component form as $x=[\delta r^t \;\; \delta v^t \;\; \phi \;\; \varepsilon]^T$.

4- 2- Measurement modeling

The radar outputs are combined with INS positions to form a measurement for processing in an onboard Kalman filter algorithm. The difference between the radar and INS measurements in the navigation frame t is expressed as:

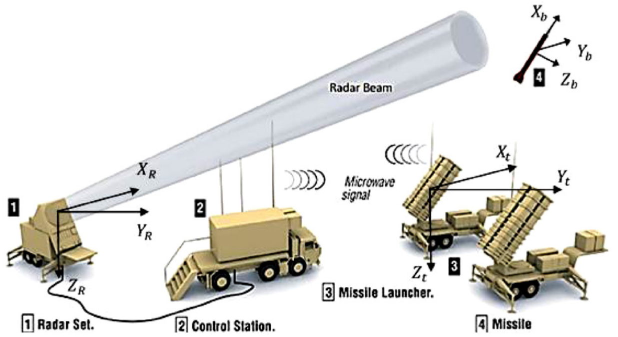

Fig. 6. Radar, navigation and body frames, background image courtesy Raytheon company copyright© 2002

$$\Delta\mathbf{r}^t = \tilde{\mathbf{r}}_{INS}^t - \tilde{\mathbf{r}}_{Radar}^t \quad (17)$$

$$\mathbf{r}_{INS} = \begin{bmatrix} x \\ y \\ z \end{bmatrix}_{INS} \quad (18)$$

where, the radar provides measurements in the polar coordinate system, i.e. the measurements of range, R, elevation, Θ, and bearing, Ψ.

Cartesian quantities may be expressed in terms of the polar coordinates as follows:

$$\mathbf{r}_{Rad} = \begin{bmatrix} x \\ y \\ z \end{bmatrix}_{Radar} = \begin{bmatrix} R\cos\Theta\cos\Psi \\ R\cos\Theta\sin\Psi \\ -R\sin\Theta \end{bmatrix}_{Radar} \quad (19)$$

Expanding Eq. (17) about a nominal position $\mathbf{r}$ and neglecting products of error quantities yields:

$$\begin{aligned} \Delta\mathbf{r}^t &= \mathbf{r}_{INS}^t + \delta\mathbf{r}_{INS}^t - \tilde{\mathbf{C}}_R^t\left(\mathbf{r}_{Radar}^R + \delta\mathbf{r}_{Radar}^R\right) \\ &= \mathbf{r}_{INS}^t + \delta\mathbf{r}_{INS}^t - \left[\mathbf{I} - (\boldsymbol{\varepsilon}\times)\right]\mathbf{C}_R^t\left(\mathbf{r}_{Radar}^R + \delta\mathbf{r}_{Radar}^R\right) \\ &= \delta\mathbf{r}_{INS}^t - \left[\left(\mathbf{C}_R^t\mathbf{r}_{Radar}^R\right)\times\right]\boldsymbol{\varepsilon} - \mathbf{C}_R^t\delta\mathbf{r}_{Radar}^R = z = \mathbf{H}x + \mathbf{M}\boldsymbol{v} \end{aligned} \quad (20)$$

where

$$\mathbf{H} = \left[\mathbf{I}_{3\times3} \;\; 0_{3\times3} \;\; 0_{3\times3} \;\; -\left\{\left(\mathbf{C}_R^t\mathbf{r}_{Radar}^R\right)\times\right\}\right]_{3\times12} \quad (21)$$

$$\mathbf{M} = \mathbf{C}_R^t \begin{bmatrix} \cos\Theta\cos\Psi & -R\sin\Theta\cos\Psi & -R\cos\Theta\sin\Psi \\ \cos\Theta\sin\Psi & -R\sin\Theta\sin\Psi & R\cos\Theta\cos\Psi \\ -\sin\Theta & -R\cos\Theta & 0 \end{bmatrix}_{Radar} \quad (22)$$

$$\boldsymbol{v} = \left[v_R \;\; v_\Theta \;\; v_\Psi\right]^T \quad (23)$$

v represents the error in the radar measurements. v is assumed to be a zero-mean, Gaussian white noise process with the covariance matrix R. $\mathbf{C}_R^t$ is a known direction cosine matrix between the radar frame and the navigation axes (t-frame). In this research, the matrix $\mathbf{C}_R^t$ is assumed time-invariant due to the fixed ground base of the radar station and the missile launcher.

5- Simulation studies

In this section, firstly the flight trajectory needed for navigation simulation is introduced. Then, the specifications of inertial sensors and the tracking radar are presented. Finally, the simulation results of INS/Radar adaptive integration navigation system are displayed and discussed.

5- 1- Flight trajectory

Fig. 7 illustrates the representative scenario used in the simulation analyses. Over the period of flight, the missile under proportional guidance laws follows a boost phase and intercepts a maneuvering target. The missile's integration inertial navigation system before second 4 is in the INS only mode and after receiving the radar data in the second 4 switches to INS/Radar mode.

5- 2- Sensor specifications

The low- cost inertial sensors specifications of INS are presented in Table 1. For the radar measurements simulation, we use the information given in Figs. 2 and 3. But, the design of an extended Kalman filter for the INS/Radar integration needs the fixed radar measurements specifications which are listed in Table 1. Also, owing to preliminary alignment between the ground-fixed radar frame and navigation frame, it is supposed that the misalignment ε is negligible.

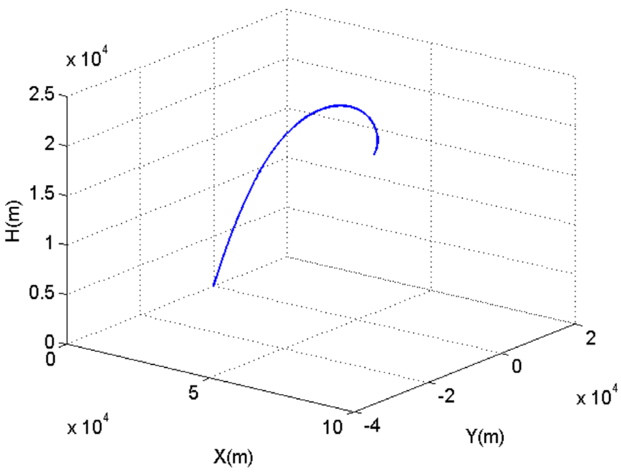

Fig. 7. The missile trajectory

Table 1. Inertial sensor and radar measurement specifications

Specification	Value (1σ)
Accelerometer In-Run Bias , *mg*	1
Accelerometer Noise Density, $\mu g / \sqrt{Hz}$	110
Gyro In-Run Bias, *deg/hr*	12
Gyro Noise Density, $(°/s)/\sqrt{Hz}$	0.015
Radar Azimuth Measurement Noise, *deg*	0.15
Radar Elevation Measurement Noise, *deg*	0.15
Radar Range Measurement Noise, *m*	12
Radar Face to Nav. Frame Misalignment, *deg*	~ 0
Radar data uplink rate, *Hz*	1

5- 3- Simulation results

Time domain Monte Carlo, MC, and the simulations of the INS/Radar integrated navigation system are carried out to compare the performance of RAE/AFKF, EKF and a new definition filter under the title of ideal EKF, IEKF. In fact, the EKF and IEKF display more or less two boundaries in the simulation results for evaluating the performance of RAE/AFKF. In the IEKF, unlike RAE/AFKF and EKF, it is supposed that the true radar measurements accuracy in every range conforming to Figs. 2 and 3 is known and the measurement noise covariance matrix of the filter is improved in every second based on this existing and virtual information. In other words, the ideal EKF can be equal to an adaptive EKF whose matrix R is only adapted and its estimation about R is definitely precise, accurate and similar to the real radar measurements accuracy, i.e. Figs. 2 and 3. Hence, the IEKF represents how good the navigation performance can be if such excellent information about the accuracies of the radar measurements is estimated and provided for the EKF disregard of the estimation method. Therefore, this virtual filter highlights the capacity of adaptive filters in the performance enhancement of INS/Radar integration navigation system.

The simulation results described below, show the standard deviations (STD) of the attitude and position errors. Each set of results has been obtained from a batch of 100 MC simulations.

Figs. 8 to 10 illustrate the standard deviation of in-flight alignment errors. These results explain that the RAE/AFKF has the superior performance in comparison with the EKF in accuracy and convergence rate. If there is the attitude error requirement of 0.2 degree (1σ), RAE/AFKF relatively satisfies it, but EKF fails to meet this supposed requirement. As shown in Figs. 8 to 10, the convergence speed of the heading and pitch alignment error is faster than those of bank alignment error. These differences are due to the dissimilar observability of these errors in data fusion process. As shown in Figs. 10, near the end of flight time, the error curves approach nearly to the same error value. This approach is due to the accelerations profile of the interceptor missile.

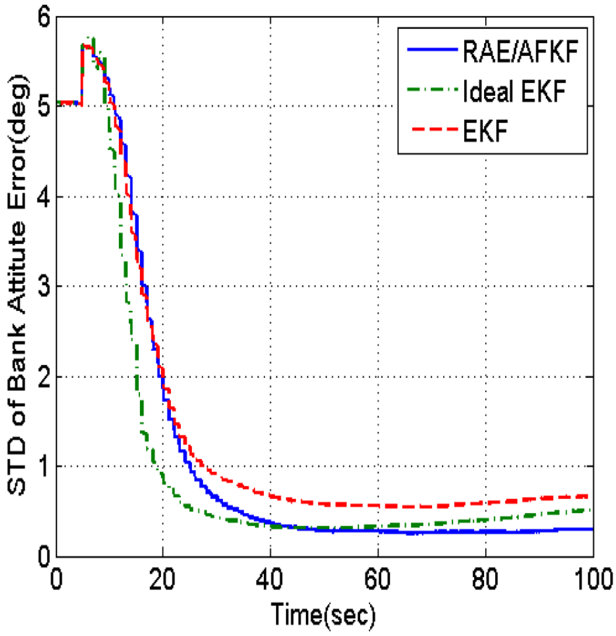

Fig. 8. STD of bank attitude error based on MC simulation

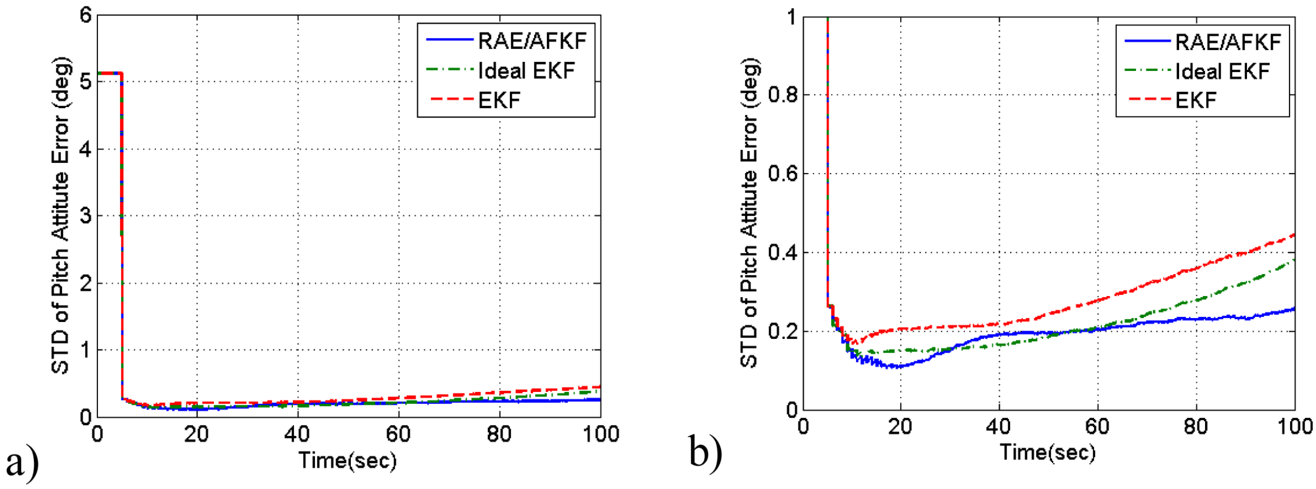

Fig. 9. STD of pitch attitude error based on MC simulation: a) all data and b) zoomed portion

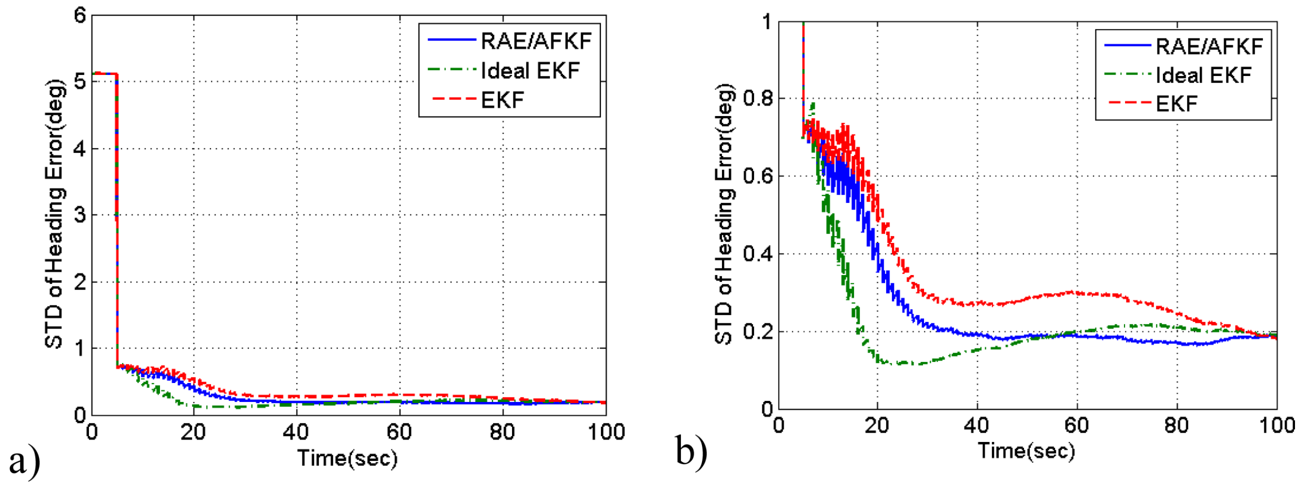

Fig. 10. STD of heading error based on MC simulation: a) all data and b) zoomed portion

The standard deviation of position errors is presented in Figs. 11 to 13. These results show that the RAE/AFKF in comparison with the EKF considerably provides more accurate navigation. Figs. 8 to 13 indicate that until nearly second 50, the performance of IEKF in accuracy and convergence rate is better than that of RAE/AFKF. It means that the accuracy of R-adaptation in the RAE/AFKF is not sufficient. However, after second 50, the navigation and alignment accuracy relevant to RAE/AFKF represent a noticeable preference over IEKF. It implies that the R-adaptation in an adaptive INS/Radar integrated navigation system is necessary for the navigation and alignment performance improvement against the radar measurements uncertainty, it but is not sufficient.

From the comparison of EKF and ideal EKF results in Figs. 8 to 13, it can be found that a proper R-adaptation in an adaptive INS/Radar integrated navigation system offers an effective tool to compensate for our insufficient prior information about the radar measurements accuracies and enhance the navigation and in-flight alignment performances as a result of the compensation. Nevertheless, in spite of the true R-adaptation in IEKF, the position error of navigation system using IEKF in final seconds is more than that of EKF as seen in Fig. 12. It denotes that the navigation error can be improved by the addition of the other adaption like P-adaption or Q-adaption.

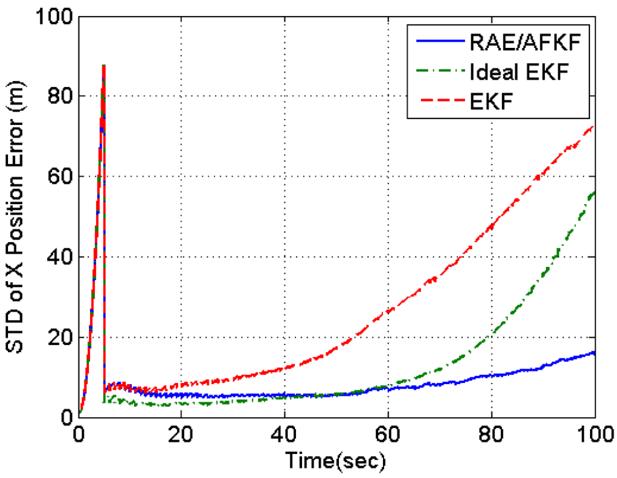

Fig. 11. STD of X position error based on MC simulation

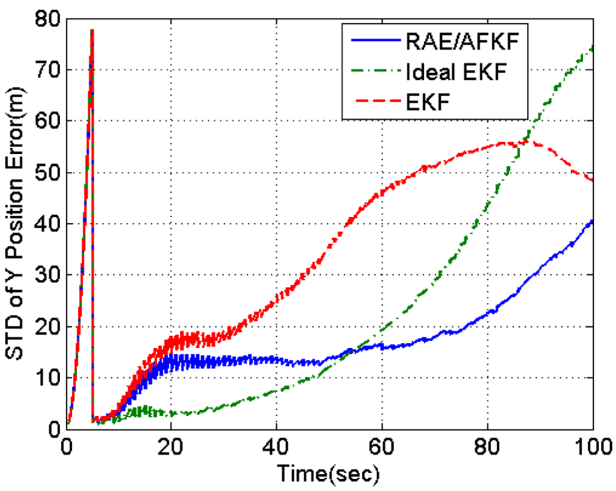

Fig. 12. STD of Y position error based on MC simulation

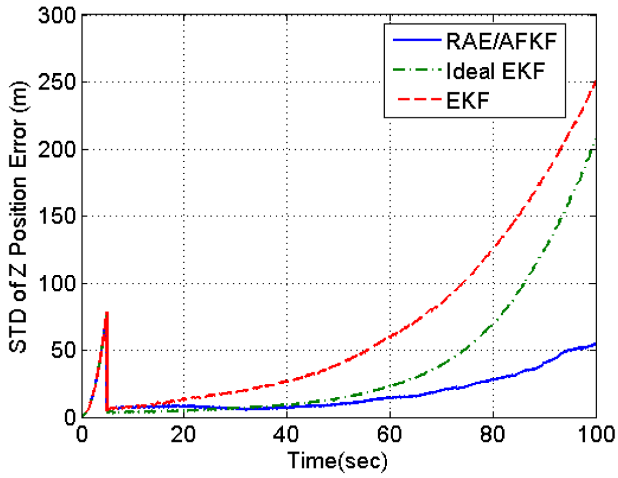

Fig. 13. STD of Z position error based on MC simulation

6- Conclusions

In this paper, a new hybrid adaptive filter based on two concepts of residual-based adaptive estimation and adaptive fading Kalman filter is proposed for the inertial navigation system/radio detection and ranging (INS/Radar) integrated navigation system. The Monte Carlo simulation results show that the presented algorithm is effective enough to improve the in-flight alignment and navigation performance in the face of the unknown and highly range-dependent accuracy of the tracking radar measurements. The proposed scheme is superior compared to the extended Kalman Filter and offers a possibility that the in-flight alignment may be achieved within a relatively short period of time. Also, this new adaptive filter puts forward a capacity that the low-cost INS/Radar integration system without aiding global navigation satellite system signals (e.g. Global Positioning System or GPS) can be used throughout the interceptor missile's mission.

7- Appendix A

Thermal noise errors of the radar angle and range measurements are random variables with the standard deviations given by respectively in degrees and meters [14, chapter 10], [15, chapters 4, 6]:

$$\sigma_{\theta_{SN}} = \frac{\theta}{k_m \sqrt{B\tau(S/N)n}} \approx \frac{\theta}{1.57\sqrt{2(S/N)n}} \quad \text{(A.1)}$$

$$\sigma_{R_{SN}} = \frac{c\tau^{0.5}}{2\sqrt{4B(S/N)n}} \quad \text{(A.2)}$$

where the free-space, and single-pulse signal-to-noise ratios (S/N) are determined using the radar range equations [14, chapter 3], [17, chapter 1]:

$$S/N = \frac{P_t G^2 \lambda^2 \sigma}{N(4\pi)^3 R^4} \quad \text{(A.3)}$$

The basic and equivalent glint error standard deviations in angle and range for uniform scattered over a target span L are given by $\sigma_{\theta_G}=L_x/3R$ and $\sigma_{R_G}=L_r/3$, respectively in degrees and meters [17, pages 115-118].

8- Appendix B

The gravity vector in t-frame in terms of the gravity vector in the local level geographic frame, n-frame, is:

$$\mathbf{g}^t = \mathbf{C}_n^t \mathbf{g}^n \quad \text{(B.1)}$$

where

$$\mathbf{g}^n = \begin{bmatrix} 0 & 0 & g \end{bmatrix}^T \quad \text{(B.2)}$$

$\mathbf{C}_n^t$ is a direction cosine matrix from n-frame to t-frame. The matrix $\mathbf{C}_n^t$ has been explained in detail in [26, page 37]. By differentiating (B.1) respect to $\mathbf{r}^t$, the gravity gradient matrix $\mathbf{G}$ is obtained as

$$\mathbf{G} = \frac{\partial \mathbf{g}^t}{\partial \mathbf{r}^t} = \frac{\partial \mathbf{C}_n^t}{\partial t}\frac{\delta t}{\delta \mathbf{r}^t}\mathbf{g}^n + \mathbf{C}_n^t \frac{\partial \mathbf{g}^n}{\partial \mathbf{r}^t} \quad \text{(B.3)}$$

where

$$\frac{\partial t}{\partial \mathbf{r}^t} = \begin{bmatrix} \frac{1}{\mathrm{v}_x} & \frac{1}{\mathrm{v}_y} & \frac{1}{\mathrm{v}_z} \end{bmatrix} \quad \text{(B.4)}$$

and for the tactical missiles, i.e. regional range, it can be supposed that

$$\frac{\partial \mathbf{g}^n}{\partial \mathbf{r}^t} \approx \begin{bmatrix} 0 & 0 & 0 \\ 0 & 0 & 0 \\ 0 & 0 & \frac{\partial g}{\partial z} \end{bmatrix} \quad \text{(B.5)}$$

Applying (B.4) to (B.3) gives:

$$\mathbf{G} = \left(\frac{g}{\mathrm{v}_z}\right)\dot{\mathbf{C}}_n^t + \mathbf{C}_n^t \frac{\partial \mathbf{g}^n}{\partial \mathbf{r}^t} \quad \text{(B.6)}$$

9- References

[1] Titterton, D. H. and Weston, J. L.; "The Alignment of Ship Launched Missile IN Systems," *Inertial Navigation Sensor Development*, IEE Colloquium on, London, 1989.

[2] Johnson, C.; Ohlmeyer, E. J. and Pepitone, T. R.; "Attitude Dilution of Precision–A New Metric for Observability of in Flight Alignment Errors," *Guidance, Navigation, and Control Conference and Exhibit*, Denver, pp. 2000–2427, 2000.

[3] Ornedo, R. S.; Farnsworth, K. A. and Sandhoo, G. S.; "GPS and Radar Aided Inertial Navigation System for Missile System Applications," *IEEE Position Location and Navigation Symposium*, Palm Spring, CA, 1998.

[4] Ohlmeyer, E. J.; Pepitone, T. R. and Hanger, D. B.; "Effect of Trajectory Shaping on Observability of NTW Interceptor In-Flight Alignment Errors," *Dahlgren VA, Naval Surface Warfare Center*, 1999.

[5] Ohlmeyer, E. J.; Hanger, D. B. and Pepitone, T. R.; "In-Flight Alignment Techniques for Navy Theater Wide Missiles," *Guidance, Navigation and Control Conference*, Montreal, 2001.

[6] Bezick, S. M.; Pue, A. J. and Patzelt, C. M.; "Inertial Navigation for Guided Missile Systems," *Johns Hopkins APL Technical Digest, Applied Physics Laboratory*, Vol. 28, pp. 331–342, 2010.

[7] Bar-Itzhack, I. Y. and Porat, B.; "Azimuth Observability Enhancement During Inertial Navigation System In-Flight Alignment," *Journal of Guidance, Control and Dynamics*, Vol. 3, No. 4, pp. 337–344, 1980.

[8] Porat, B. and Bar-Itzhack, I. Y.; "Effect of Acceleration Switching During INS In-Flight Alignment," *Journal of Guidance, Control and Dynamics*, Vol. 4, No. 4, pp. 385–389, 1981.

[9] Bar-Itzhack, I. Y.; "Minimal Order Time Sharing Filters for INS In-Flight Alignment," *Journal of Guidance, Control and Dynamics*, Vol. 5, No. 4, pp. 396–402, 1982.

[10] Anders, J. L.; Johnson, C.; Luckau, A. M.; Moore, T. A. and Ornedo, R. S.; "Successful Flight Test of a GPS and Radar Aided Inertial Navigation System," *Proceedings of the National Technical Meeting of The Institute of Navigation*, San Diego, CA, 2002.

[11] Anders, J. L.; Buhar, C.; Estrada, V.; Johnson, C. and Ornedo, R. S.; "New Generation GPS and Radar Aided Inertial Navigation System for Ballistic Missile Interceptor," *Procedings of the 60th Annual Meeting of The Institute of Navigation*, Dayton OH, 2004.

[12] Gul, F.; Fang, J. and Khan, S.; "SINS Augmentation by ANS and Secure Radio Positioning System," *2nd International Conference on Emerging Technologies (ICET)*, pp. 278–284, 2006.

[13] Li, S. and Peng, Y.; "Radio Beacons/IMU Integrated Navigation for Mars Entry," *Advances in Space Research*, Vol. 47, No. 7, pp. 1265–1279, 2011.

[14] Barton, D. K.; "Radar Evaluation Handbook," *Artech House*, Norwood MA, 1991.

[15] Skolnik, M. I.; "Introduction to Radar Systems," *McGraw Hill*, New York, 3rd Edition, 2001.

[16] Mohamed, A. H. and Schwarz, K. P.; "Adaptive Kalman Filtering for INS/GPS," *J. Geodesy*, Vol. 73, No. 4, pp. 193–203. 1999.

[17] Barton, D. K.; "Modern Radar System Analysis," *Artech House*, Norwood, MA, 1988.

[18] Ewell, G. W.; Alexander, N. T. and Tomberlin, E. L.; "Investigation of Target Tracking Errors in Monopulse Radars," *Georgia Institute of Technology*, Atlanta, Georgia, 1972.

[19] Barton, D. K. and Barton, W. F.; "Modern Radar System Analysis Software and User's Manual Version 2.0," *Artech House*, Norwood MA, 1993.

[20] Jwo, D. J.; Chung, F. C. and Weng, T. P.; "Adaptive Kalman Filter for Navigation Sensor Fusion," *Sensor Fusion and its Applications*, Shanghai, InTech, pp. 65–91, 2001.

[21] Hide, C.; Moore, T. and Smith, M.; "Adaptive Kalman Filtering for Low-Cost INS/GPS," *The Journal of Navigation*, Vol. 56, Vol. 1, pp. 143–152, 2003.

[22] Xia, Q.; Rao, M.; Ying, Y. and Shen, X.; "Adaptive Fading Kalman Filter with an Application," *Automatica*, Vol. 30, No. 8, pp. 1333–1338, 1994.

[23] Jwo, D. J. and Weng, T. P.; "An Adaptive Sensor Fusion Method with Applications in Integrated Navigation," *The Journal of Navigation*, Vol. 61, No. 4, pp. 705–721, 2008.

[24] Simon, D.l "Optimal State Estimation," *John Wiley and Sons*, Hoboken, New Jersey, 2006.

[25] Titterton, D. H. and Weston, J. L.; "Strapdown Inertial Navigation Technology," *Peter Peregrinus*, London, 1997.

[26] Britting, K. R.; "Inertial Navigation Systems Analysis," *John Wiley and Sons Inc.*, USA, 1971.